

Energy flow between two hydrodynamically coupled particles kept at different effective temperatures

A. BÉRUT, A. PETROSYAN, S. CILIBERTO

Université de Lyon
Laboratoire de Physique, École Normale Supérieure de Lyon, CNRS UMR5672
46, Allée d'Italie, 69364 Lyon Cedex 07, France

PACS 05.40.-a – Fluctuation phenomena, random processes, noise, and Brownian motion
 PACS 82.70.Dd – Colloids
 PACS 87.80.Cc – Optical trapping

Abstract –We measure the energy exchanged between two hydrodynamically coupled micron-sized Brownian particles trapped in water by two optical tweezers. The system is driven out of equilibrium by random forcing the position of one of the two particles. The forced particle behaves as it has an “effective temperature” higher than that of the other bead. This driving modifies the equilibrium variances and cross-correlation functions of the bead positions: we measure an energy flow between the particles and an instantaneous cross-correlation, proportional to the effective temperature difference between the two particles. A model of the interaction which is based on classical hydrodynamic coupling tensors is proposed. The theoretical and experimental results are in excellent agreement.

The energy flux between two micro-systems kept at different temperatures and coupled only by thermal fluctuations plays an important role in out of equilibrium thermodynamics. For this reason it has been widely studied theoretically [1–9], but only a few experiments [10,11] have analyzed this problem. Furthermore in all of these studies the systems where coupled by conservative forces and the dissipative coupling have never been considered. This is however a very important case because the coupling of two close Brownian particles is dominated by their hydrodynamic interactions in low Reynold-number regimes. These interactions, which have been widely studied in fluid at thermal equilibrium starting from hydrodynamic calculations [12–14], play an important role in various physical situations. For example, the indirect interactions mediated by the solvent modify the Brownian diffusion of two particles [15,16], and gives rise to an anti-correlation at finite time between the displacements of two trapped particles, which has been studied both experimentally and numerically [17–20]. Systems with arrays of more than two trapped particles coupled by hydrodynamic interactions show complex dynamics and can behave as an elastic medium [21–24]. The hydrodynamic coupling is also responsible for the synchronisation of colloidal oscillators which can be linked to collective motions of biological

systems like cilia or flagella [25–28], and for the pair-attractions of particles driven on a circular ring [29,30]. Despite the variety of situations, the interactions between particles trapped at different temperatures were not studied, due to the difficulty of achieving a high temperature difference on very small scales.

The purpose of this letter is to study how the equilibrium statistical properties are modified by the hydrodynamic coupling between two particles trapped at different effective kinetic temperatures. The main results of our investigation concern the energy flux and the positions correlation functions. The experimental results are compared to those of an analytical model based on classical hydrodynamic coupling tensor. The “effective temperature difference” is produced by random forcing the positions of one of the two particles. This is a technique that have been used in two experiments on single particle, which have shown that the random forcing can be indeed assimilated to an “effective temperature” [31,32].

In order to study these non-equilibrium interactions we use the following experimental setup: a laser beam (wavelength 532nm) is separated in two beams with crossed polarizations so that there is no interference between them. A custom-built vertical optical tweezers with an oil-immersion objective (HCX PL. APO 63×/0.6-1.4) is

used to focus each beam which creates a quadratic potential well where a silica bead (radius $R = 1 \mu\text{m} \pm 5\%$) is trapped. One of the beams goes through an acousto-optic deflector (AOD) that allows to switch the position of the trap very rapidly (up to 1 MHz). The beads are dispersed in bidistilled water at low concentration to avoid interactions with multiple other beads. The solution of beads is contained in a disk-shaped cell (18 mm in diameter, 1 mm in depth). The beads are trapped at $15 \mu\text{m}$ above the bottom surface of the cell. The position of the beads is tracked by a fast camera with a resolution of 115 nm per pixel, which after treatment gives the position with an accuracy greater than 5 nm. The trajectories of the bead are sampled at 800 Hz. The stiffness of the traps k is proportional to the laser intensity¹ and is typically about 4 pN/ μm . The two particles are trapped on a line (called “x axis”) and separated by a distance d which is tunable. For all the distances used (between 2.8 and 6 μm) the Coulombian interaction between the particle surfaces is negligible.

The stiffness of one trap at equilibrium can be measured by calculating the variance of the x-displacement of the bead σ_x^2 which, because of energy equipartition, is equal to $\frac{k_B T}{k}$ where k_B is the Boltzmann constant and T the temperature. Equivalently the power spectrum of the x-displacement is Lorentzian since the particles are over-damped: $S(f) = \frac{2\gamma k_B T / k^2}{1 + f^2 / f_c^2}$, and one can fit it to find the cut-off frequency f_c that verifies $f_c = \frac{k}{2\pi\gamma}$ where $\gamma = 6\pi R\eta$ and η is the dynamic viscosity of water. The two methods give compatible results (assuming the viscosity of water and corrections due to the finite distance between the particle and the bottom of the cell are known).

To create an effective temperature on one of the particles (for example on particle 1), a Gaussian white noise is sent to the AOD so that the position of the corresponding trap is moved randomly in the direction where the particles are aligned. If the amplitude of the displacement is sufficiently small to stay in the linear regime it creates a random force on the particles which does not affect the stiffness of the trap. Here the particles are over-damped and have a Lorentzian power spectrum with a typical cut-off frequency f_c of 30 Hz. The added noise is numerically created by a LABVIEW program: it is sampled at 100 kHz with a tunable amplitude A (typically of ~ 1 V) and numerically low-pass filtered at 1 kHz. It is then generated by the analog output of a NI PXIe-6366 card. The conversion factor for the displacement due to the AOD is $2.8 \mu\text{m}/\text{V}$, and the typical voltage of the noise after filtration is between ± 0.25 V. When the random force is switched on, the bead quickly reaches a stationary state with an “effective temperature” for the randomly forced degree of freedom.

The power spectra of one bead’s displacement in the x-direction with different noise amplitude (between 0 and

1.8 V) are shown in fig.1. The displacement in the y-direction is not modified by the added noise.

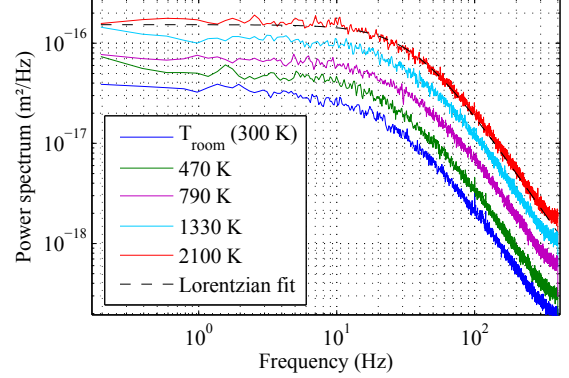


Fig. 1: Power spectra of the x-displacement of one bead of radius $R = 1 \mu\text{m}$ trapped with stiffness $k = 3.4 \text{ pN}/\mu\text{m}$ in water at room temperature, at equilibrium (lowest blue curve), and for noise amplitude A from 0.6 to 1.8 V (A is incremented of 0.4 V between each curve). The black dashed line is a Lorentzian fit of the spectrum with $A = 1.8$ V. The indicated effective temperatures are calculated from the change of variance because the stiffness and viscosity are not modified by the forcing.

As in [31], the power spectra when the bead is randomly forced are just vertical translations of the equilibrium one, which shows that only the effective temperature is modified (and not the stiffness of the trap, nor the viscosity of water). The cut-off frequency obtained by fitting the power spectra is not modified by more than a few hertz when the amplitude of the forcing is lower than 1.5 V. For higher forcing amplitude, f_c starts to be modified and the spectrum starts to be slightly less accurate at high frequency. This happens because the forced random displacement of the trap is too big compared to the size of the harmonic interval of the trapping potential.

This setup allows us to create a wide range of effective temperatures for one bead, and to look at the interaction between this agitated bead and another one trapped at equilibrium at a finite distance d .

When the first bead is forced we observe that the variance of its x-displacement $\sigma_{11}^2 = \langle x_1 x_1 \rangle$ increases, which corresponds to the effect of the random forcing. The variance of the second particle’s displacement $\sigma_{22}^2 = \langle x_2 x_2 \rangle$ is also increased due to the coupling between the two particle, and more surprisingly the cross-variance $\sigma_{12}^2 = \langle x_1 x_2 \rangle$ (which is the instantaneous cross-correlation of the x-displacements) ceases to be zero and increases with the amplitude of the random noise (see fig. 2(a)). For a fixed noise amplitude, the values of σ_{22}^2 and σ_{12}^2 also slightly decrease with the distance d between the particles (see fig. 2(b)).

To understand this behaviour, we can use the classical hydrodynamic coupling. Following [17–19] the motion of

¹It can be modified by turning an half-wave plate placed before the polarization separation or by adding neutral density filters on the beams trajectory.

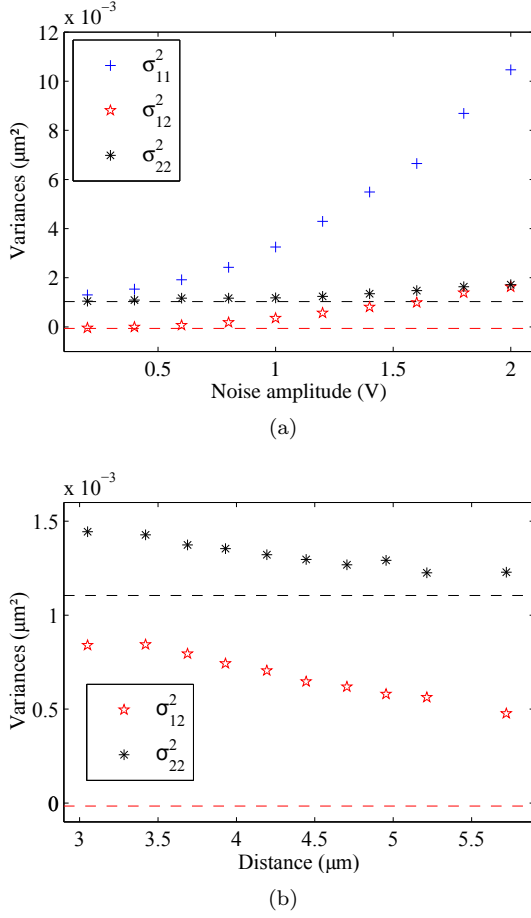


Fig. 2: Variance of the displacement of each bead (σ_{22}^2 and σ_{11}^2) and cross-variance between the two displacement (σ_{12}^2). (a) When the random forcing amplitude A is increased on the first bead and the distance between the traps is kept constant, $d = 3.2 \mu\text{m}$, the variances and the cross-variance increase. The dashed-lines are the values of σ_{22}^2 and σ_{12}^2 measured when there is no random forcing. (b) Zoom on σ_{22}^2 and σ_{12}^2 for a fixed forcing amplitude $A = 1.5 \text{ V}$, both values decrease with d the mean distance between the two particles (σ_{11}^2 which is not shown remains nearly constant and equal to $5.7 \times 10^{-3} \mu\text{m}^2$). The dashed-lines are the values of σ_{22}^2 and σ_{12}^2 averaged over d when there is no random forcing.

two identical particles of radius R trapped at positions separated by a distance d is described by two coupled Langevin equations:

$$\begin{pmatrix} \dot{x}_1 \\ \dot{x}_2 \end{pmatrix} = \mathcal{H} \times \begin{pmatrix} F_1 \\ F_2 \end{pmatrix} \quad (1)$$

where \mathcal{H} is the hydrodynamic coupling tensor, x_i is the position of the particle i relative to its trapping position and F_i is the force acting on the particle i .

In the case where the displacements are small compared to the mean distance between the particles, the hydrody-

namic coupling tensor reads:

$$\mathcal{H} = \begin{pmatrix} 1/\gamma & \epsilon/\gamma \\ \epsilon/\gamma & 1/\gamma \end{pmatrix} \quad (2)$$

where γ is the Stokes friction coefficient ($\gamma = 6\pi R\eta$ where η is the viscosity of water) and ϵ is the coupling coefficient ($\epsilon = \frac{3R}{2d}$ if one takes the first order of the Oseen tensor [33], $\epsilon = \frac{3R}{2d} - \left(\frac{R}{d}\right)^3$ if one takes the Rotne-Prager diffusion tensor [24]).

At equilibrium the forces acting on the particles are:

$$F_i = -k_i \times x_i + f_i \quad (3)$$

where k_i is the stiffness of the trap i and f_i are the Brownian random forces which verify:

$$\begin{aligned} \langle f_i(t) \rangle &= 0 \\ \langle f_i(t) f_j(t') \rangle &= 2k_B T (\mathcal{H}^{-1})_{ij} \delta(t - t') \end{aligned} \quad (4)$$

where k_B is the Boltzmann constant and T the temperature of the surrounding fluid.

Here we simply add an external random force f^* on the first particle. This force is completely decorrelated with the Brownian random forces and characterised by an additional effective temperature ΔT (the particle 1 is then at an effective temperature $T^* = T + \Delta T$).

$$\begin{aligned} \langle f^*(t) \rangle &= 0 \quad \text{and} \quad \langle f^*(t) f_i(t') \rangle = 0 \\ \langle f^*(t) f^*(t') \rangle &= 2k_B \Delta T \gamma \delta(t - t') \end{aligned} \quad (5)$$

It follows that the system of equations is:

$$\begin{cases} \gamma \dot{x}_1 = -k_1 x_1 + \epsilon(-k_2 x_2 + f_2) + f_1 + f^* \\ \gamma \dot{x}_2 = -k_2 x_2 + \epsilon(-k_1 x_1 + f_1 + f^*) + f_2 \end{cases} \quad (6)$$

It can be rewritten:

$$\begin{cases} \dot{x}_1 = g_1(x_1, x_2) + \xi_1 \\ \dot{x}_2 = g_2(x_1, x_2) + \xi_2 \end{cases} \quad (7)$$

with:

$$\begin{aligned} g_i(x_i, x_j) &= -\frac{1}{\gamma} k_i x_i - \frac{\epsilon}{\gamma} k_j x_j \\ \xi_1 &= \frac{1}{\gamma} (f_1 + \epsilon f_2 + f^*) \\ \xi_2 &= \frac{1}{\gamma} (f_2 + \epsilon f_1 + \epsilon f^*) \end{aligned} \quad (8)$$

The equations are close to those describing the energy exchanged between two heat baths coupled by thermal fluctuations [10] and it can be proved that the time evolution of the joint probability distribution function (PDF) $P(x_1, x_2, t)$ is governed by the Fokker-Planck equation [34]:

$$\begin{aligned} \frac{\partial P}{\partial t} = & -\frac{\partial(g_1 P)}{\partial x_1} - \frac{\partial(g_2 P)}{\partial x_2} + 2\theta_{12} \frac{\partial^2 P}{\partial x_1 \partial x_2} \\ & + \theta_{11} \frac{\partial^2 P}{\partial x_1^2} + \theta_{22} \frac{\partial^2 P}{\partial x_2^2} \end{aligned} \quad (9)$$

where θ_{ij} is defined by:

$$\langle \xi_i(t) \xi_j(t') \rangle = 2\theta_{ij} \delta(t - t') \quad (10)$$

Here we have:

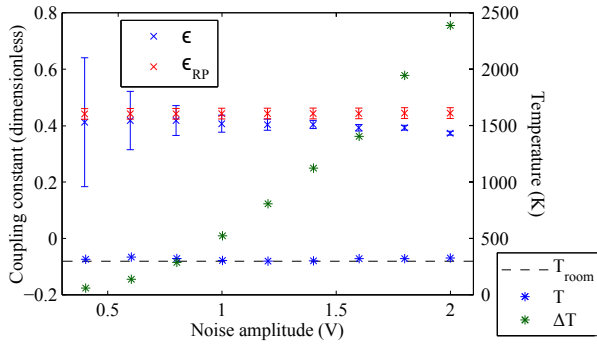
$$\begin{aligned}\theta_{11} &= k_B(T + \Delta T)/\gamma \\ \theta_{12} &= k_B\epsilon(T + \Delta T)/\gamma \\ \theta_{22} &= k_B(T + \epsilon^2\Delta T)/\gamma\end{aligned}\quad (11)$$

The stationary solution of equation 9 can be written:

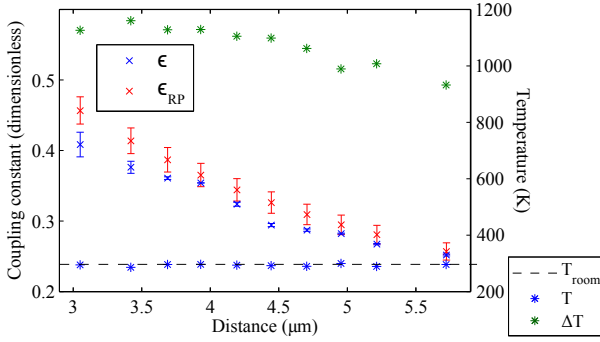
$$P_s(x_1, x_2) = \frac{\sqrt{ac - b^2}}{\pi} e^{-(ax_1^2 + 2bx_1x_2 + cx_2^2)} \quad (12)$$

where

$$\begin{aligned}a &= \frac{k_1(k_1 + k_2)((k_1 + k_2)T + \epsilon^2 k_2 \Delta T)}{2k_B((T^2 + T\Delta T)(k_1 + k_2)^2 - \epsilon^2(\epsilon^2 - 1)k_2^2 \Delta T^2)} \\ b &= \frac{-\epsilon k_1 k_2 (k_1 + k_2) \Delta T}{2k_B((T^2 + T\Delta T)(k_1 + k_2)^2 - \epsilon^2(\epsilon^2 - 1)k_2^2 \Delta T^2)} \\ c &= \frac{k_2(k_1 + k_2)((k_1 + k_2)T + (k_1 + k_2(1 - \epsilon^2))\Delta T)}{2k_B((T^2 + T\Delta T)(k_1 + k_2)^2 - \epsilon^2(\epsilon^2 - 1)k_2^2 \Delta T^2)}\end{aligned}\quad (13)$$



(a)



(b)

Fig. 3: Coupling coefficient (ϵ), temperature of the bath (T) and effective temperature (ΔT), measured from the values of $\sigma_{11}^2, \sigma_{12}^2$ and σ_{22}^2 , and theoretical coupling coefficient from the Rotne-Prager diffusion tensor (ϵ_{RP}) for particles of radius $R = 1 \mu\text{m} \pm 5\%$. (a) For two particles trapped at distance $d = 3.2 \mu\text{m}$ as a function of the amplitude A of the forcing done on one particle. (b) For two particles at different effective temperature as a function of the distance d between the particles.

Then, one can compute the variances of each position and the cross-variance between the two particles:

$$\begin{aligned}\sigma_{11}^2 &= \langle x_1 x_1 \rangle = \frac{k_B(T + \Delta T)}{k_1} - \frac{k_2}{k_1} \frac{\epsilon^2 k_B \Delta T}{k_1 + k_2} \\ \sigma_{12}^2 &= \langle x_1 x_2 \rangle = \frac{\epsilon k_B \Delta T}{k_1 + k_2} \\ \sigma_{22}^2 &= \langle x_2 x_2 \rangle = \frac{k_B T}{k_2} + \frac{\epsilon^2 k_B \Delta T}{k_1 + k_2}\end{aligned}\quad (14)$$

This result shows the appearance of the non-zero cross-variance which does not exist in the equilibrium case, and an exchange of energy between the two particles. Indeed the variances can be rewritten $\sigma_{11}^2 = \sigma_{11, \text{n.c.}}^2 - \frac{k_2}{k_1} \frac{\epsilon^2 k_B \Delta T}{k_1 + k_2}$ and $\sigma_{22}^2 = \sigma_{22, \text{n.c.}}^2 + \frac{\epsilon^2 k_B \Delta T}{k_1 + k_2}$ where $\sigma_{i, \text{n.c.}}^2$ is the variance of the particle i with no coupling. It follows that the variance of the “hot” particle (the forced one) is decreased by the presence of the “cold” particle, and reciprocally the variance of the cold one is increased by the presence of the hot one.

By measuring $\sigma_{11}^2, \sigma_{12}^2$ and σ_{22}^2 , one can solve the system 14 and find the values of T , ΔT and ϵ (given that k_1 and k_2 are measured separately). Some experimental values for a given distance d and different amplitudes of forcing A done on the particle 1 are shown in figure 3(a), and for a given forcing amplitude and different distances are shown in figure 3(b). As expected, T is always nearly constant and equal to room temperature (all values are compatible with room temperature of 297 K with a precision of 10%), ϵ depends only on the distance between the particles (in figure 3(a) all values are between 0.37 and 0.42), and ΔT depends only on the forcing amplitude done on the first particle.

In fig. 3(a) and 3(b) we notice that the measured value of ϵ is always slightly lower than the theoretical one (estimated by the Rotne-Prager diffusion tensor) but shows the same dependence in the distance d between the two particles.² Note that there are two experimental problems : a) for very low forcing (i.e. low ΔT), the errorbars on ϵ are big because they are estimated considering that the main source of incertitude is the value of σ_{12}^2 , which is very low when forcing is low.³ b) when the forcing is very high, the estimation of ϵ starts to be less precise because, as already mentioned, the added random force begins to be less accurate for high displacements of the trap position. In fig. 3(b) also the effective temperature ΔT slightly decreases when the distance d is increased because of the less accurate response of the AOD far from the center of the apparatus⁴.

It is interesting to notice that the values of $\sigma_{11}^2, \sigma_{12}^2$ and σ_{22}^2 are linked to the mean heat flux between the two particles. Indeed the heat dissipated⁵ by the particle i during the time τ is given by [35]:

$$Q_i(\tau) = \int_0^\tau (\gamma \dot{x}_i - \gamma \xi_i) \dot{x}_i dt \quad (15)$$

²For this discrepancy it has been verified that the value of ϵ is not significantly modified if the distance between the bead and the bottom surface of the cell is changed to 10 μm or 20 μm .

³Here the values of σ_{12}^2 used for computation are corrected by subtracting the value of the cross-variance when the system is at equilibrium (this value should theoretically be zero and gives an estimation of the incertitude on σ_{12}^2).

⁴The shape of the trap is always impaired when the beam is not well centred, which lowers the stiffness of the trap and the ΔT corresponding to a given noise amplitude.

⁵In the published version we have written “received” but it was a mistake.

Using equations 7 it can be decomposed in two terms:

$$Q_i(\tau) = k_i q_{ii} + \epsilon k_j q_{ij} \quad (16)$$

Where:

$$\begin{aligned} q_{ii} &= -\int_0^\tau x_i \dot{x}_i dt \\ q_{ij} &= -\int_0^\tau x_j \dot{x}_i dt \end{aligned} \quad (17)$$

The average of the two terms q_{22} and q_{21} contributing to Q_2 , integrated over 1 s, are shown figure 4 for different effective temperatures ΔT . These values are very close to the opposite of the terms contributing to Q_1 . The maximal difference between $-\langle q_{12} \rangle$ and $\langle q_{21} \rangle$ is of 0.24 % and both terms depends linearly on ΔT . Moreover, the terms $\langle q_{11} \rangle$ and $\langle q_{22} \rangle$ are always nearly equal to zero (the maximal value observed is $6 \times 10^{-16} \mu\text{m}^2$), which is normal since $\int_0^\tau -x_i \dot{x}_i dt = -[\frac{1}{2}x_i^2]_0^\tau$. Then the mean heat dissipated by particle i during time τ is:

$$\langle Q_i(\tau) \rangle = \epsilon k_j \langle q_{ij} \rangle \quad (18)$$

It follows that the mean dissipated heat by particle 1 and received heat by particle 2 are proportional to ΔT as would be a normal mean heat flux between two sources at different temperatures. This result allows us to interpret the cross-variance σ_{12}^2 and the difference $\sigma_{ii}^2 - \sigma_{i.n.c.}^2$, which also depend linearly on ΔT , as proportional to the heat flux going from the particle 1 (“hot”) to the particle 2 (“cold”).

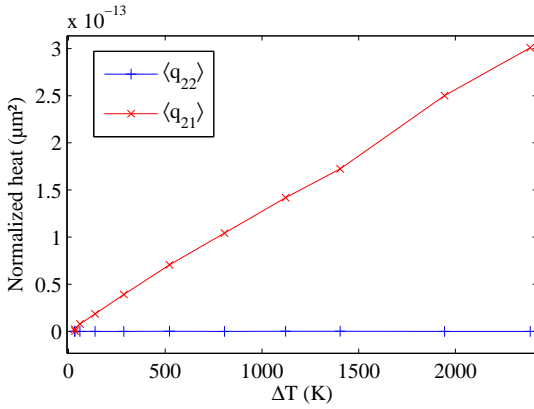


Fig. 4: Mean normalized heat received by particle 2 during a time $\tau = 1$ s ($d = 3.2 \mu\text{m}$). The average is done on 500 independent portions of trajectories. The mean normalized heat dissipated by particle 1 is not shown because the curves are too close to be differentiated.

Finally, following the resolution method described in [19] and using the eqs. 14, one can compute the cross-correlation functions of x_1 and x_2 for time t ($t > 0$):

$$\begin{aligned} \langle x_1(t)x_2(0) \rangle &= \frac{\epsilon k_B}{2(k_1+k_2)\kappa} \times \\ &\left[(\Delta T(\kappa+k_1+k_2(2\epsilon^2-1))+2T(k_1+k_2))e^{-\frac{((k_1+k_2)-\kappa)t}{2\gamma}} \right. \\ &\left. + (\Delta T(\kappa-k_1-k_2(2\epsilon^2-1))-2T(k_1+k_2))e^{-\frac{((k_1+k_2)+\kappa)t}{2\gamma}} \right] \end{aligned} \quad (19)$$

$$\begin{aligned} \langle x_1(0)x_2(t) \rangle &= \frac{\epsilon k_B}{2(k_1+k_2)\kappa} \times \\ &\left[(\Delta T(\kappa+k_1+k_2(3-2\epsilon^2))+2T(k_1+k_2))e^{-\frac{((k_1+k_2)-\kappa)t}{2\gamma}} \right. \\ &\left. + (\Delta T(\kappa-k_1-k_2(3-2\epsilon^2))-2T(k_1+k_2))e^{-\frac{((k_1+k_2)+\kappa)t}{2\gamma}} \right] \end{aligned} \quad (20)$$

with :

$$\kappa = \sqrt{k_1^2 - 2k_1k_2 + k_2^2 + 4\epsilon^2k_1k_2} \quad (21)$$

When $k_1 = k_2 = k$ the expressions can be simplified:

$$\langle x_1(t)x_2(0) \rangle = \frac{k_B}{4k} \times \left[(-2T + \Delta T\epsilon(1-\epsilon))e^{-\frac{k(1-\epsilon)t}{\gamma}} + (2T + \Delta T\epsilon(1+\epsilon))e^{-\frac{k(1+\epsilon)t}{\gamma}} \right] \quad (22)$$

$$\begin{aligned} \langle x_1(0)x_2(t) \rangle &= \frac{k_B}{4k} \times \\ &\left[(-2T + \Delta T(-2+\epsilon+\epsilon^2))e^{-\frac{k(1-\epsilon)t}{\gamma}} + \right. \\ &\left. (2T + \Delta T(2+\epsilon-\epsilon^2))e^{-\frac{k(1+\epsilon)t}{\gamma}} \right] \end{aligned} \quad (23)$$

Of course if $\Delta T = 0$, $\langle x_1(0)x_2(t) \rangle$ and $\langle x_1(t)x_2(0) \rangle$ are equal because the two beads play the same role and the expressions become the same as the ones obtained in [17–19]. The theoretical expressions of the cross-correlation functions can be compared with the experimental data since all parameters can be measured. The results are shown figure 5. The data show a good agreement with the model. Since the values of k_1 and k_2 are nearly equal (for the data shown figure 5: $k_1 \simeq 3.4 \text{ pN}/\mu\text{m}$ and $k_2 \simeq 4.0 \text{ pN}/\mu\text{m}$) there is no big difference between the curves obtained from eqs. 19–20 (green curves) and those obtained from eqs. 22–23 using for k the mean value of k_1 and k_2 (red curves). Note that, contrary to the equilibrium case, $\langle x_1(0)x_2(t) \rangle$ and $\langle x_1(t)x_2(0) \rangle$ are not equal, since the roles of particles 1 and 2 are not symmetrical. $\langle x_1(0)x_2(t) \rangle$ always shows a time-delayed anti-correlations more pronounced than in the equilibrium case whereas $\langle x_1(t)x_2(0) \rangle$ doesn’t show any anti-correlation as soon as $\Delta T \geq \frac{2}{\epsilon(1-\epsilon)}T$. This behaviour can be understood in the following way: $\langle x_i(0)x_j(t) \rangle$ is linked to the influence that x_i at a given time $t = 0$ has on x_j after a time t . Since x_1 is forced, it is less sensitive to the motion of x_2 , whereas x_2 is more sensitive to the motion of x_1 which is bigger than its own motion.

In conclusion, we have shown that the random forcing of the position of trapped bead does not modifies the trap stiffness and it can be interpreted as an effective temperature for the bead. This effective temperature has been used to study the energy fluxes and the correlations functions between two particles at different temperatures and coupled only by hydrodynamic interactions. The main result of this letter is that these interactions, simply described by the classical hydrodynamic coupling tensor, gives rise to an unusual instantaneous cross-correlation between the motions of the particles and an effective energy exchange from the hot bead to the cold bead, which are

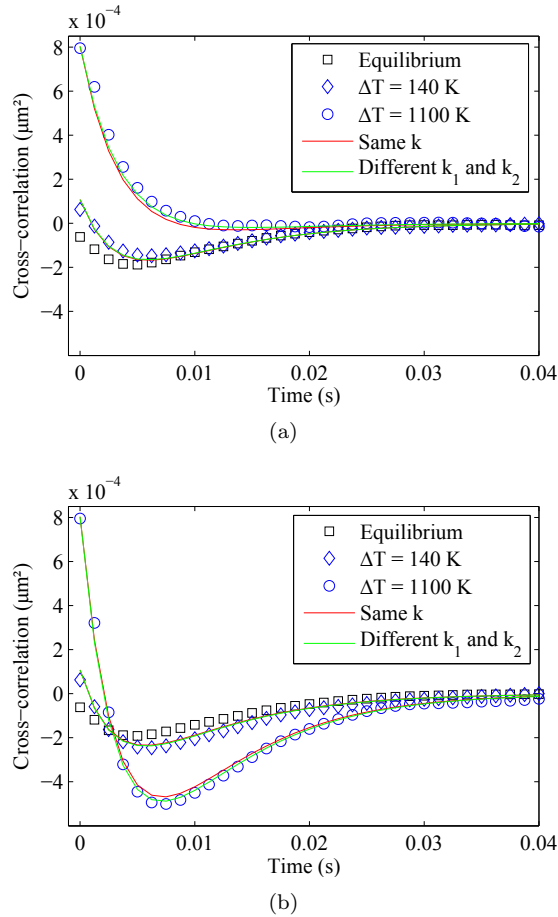


Fig. 5: Measured cross-correlations compared to the theoretical expressions with measured parameters, by taking account of the slightly different values of k_1 and k_2 (green) or considering a unique mean value for the two stiffness $k_1 = k_2 = k$ (red). (a) $\langle x_1(t)x_2(0) \rangle$. (b) $\langle x_1(0)x_2(t) \rangle$.

proportional to the mean heat flux between the two particles. The experimental results are in very good agreement with the prediction of a theoretical model based on the resolution of two coupled Langevin equations, using equivalent Fokker-Planck equations.

REFERENCES

- [1] BODINAU T. and DERIDDA B., *Phys. Rev. Lett.*, **92** (2004) 180601
- [2] JARZYNSKI C. and WŁOJCİK D. K., *Phys. Rev. Lett.*, **92** (2004) 230602
- [3] VAN DEN BROECK C., KAWAI R. and MEURS P., *Phys. Rev. Lett.*, **93** (2004) 090601
- [4] VISCO P., *J. Stat. Mech.*, **06** (2006) P06006
- [5] SAITO K. and DHAR A., *Phys. Rev. Lett.*, **99** (2007) 180601
- [6] ANDRIEUX D., GASPARD P., MONNAI T. and TASAKI S., *New J. Phys.*, **11** (2009) 043014
- [7] EVANS D., SEARLES D. J. and WILLIAMS S. R., *J. Chem. Phys.*, **132** (2010) 024501
- [8] CAMPISI M., TALKNER P. and HÄNGGI P., *Rev. Mod. Phys.*, **83** (2011) 771
- [9] CRISANTI A., PUGLISI A. and VILLAMAINA D., *Phys. Rev. E*, **85** (2012) 061127
- [10] CILIBERTO S., IMPARATO A., NAERT A. and TANASE M., *J. Stat. Mech.*, **12** (2013) P12014
- [11] KOSKI J. V., SAGAWA T., SAIRA O.-P., YOON Y., KUTVONEN A., SOLINAS P., MÖTTÖNEN M., ALANISSILA T. and PEKOLA J. P., *Nature Physics*, **9** (2013) 644
- [12] STIMSON M. and JEFFERY G. B., *Proc. Roy. Soc.*, **111** (1926) 110
- [13] BATCHELOR G. K., *J. Fluid Mech.*, **74** (1976) 1
- [14] JEFFREY D. J. and ONISHI Y., *J. Fluid. Mech.*, **139** (1984) 261
- [15] CROCKER J. C., *J. Chem. Phys.*, **106** (1997) 2837
- [16] DUFRESNE E. R., SQUIRES T. M., BRENNER M. P. and GRIER D. G., *Phys. Rev. Lett.*, **85** (2000) 3317
- [17] MEINERS J.-C. and QUAKE S. R., *Phys. Rev. Lett.*, **82** (1999) 2211
- [18] BARTLETT P., HENDERSON S. I. and MITCHELL S. J., *Phil. Trans. R. Soc. Lond. A*, **359** (2001) 883
- [19] HOUGH L. A. and OU-YANG H. D., *Phys. Rev. E*, **65** (2002) 021906
- [20] DONG-HUI H., TAO Y., WEI-HUA L., QING-LAN Z. and HONG-RU M., *Chinese Phys.*, **16** (2007) 3138
- [21] POLIN M., GRIER D. G. and QUAKE S. R., *Phys. Rev. Lett.*, **96** (2006) 088101
- [22] DI LEONARDO R., KEEN S., LEACH J., SAUNTER C. D., LOVE G. D., RUOCCO G. and PADGETT M. J., *Phys. Rev. E*, **76** (2007) 061402
- [23] CICUTA G. M., KOTAR J., BROWN A. T., NOH J.-H. and CICUTA P., *Phys. Rev. E*, **81** (2010) 051403
- [24] HERRERA-VELARDE S., EUÁN-DÍAZ E. C., CÓRDOBA-VALDÉS F. and CASTAÑEDA-PRIEGO R., *J. Phys.: Condens. Matter*, **25** (2013) 325102
- [25] KOTAR J., LEONI M., BASSETTI B., COSENTINO LAGO-MARSINO M. and CICUTA P., *Proc. Natl Acad. Sci. USA*, **107** (2010) 7669
- [26] CURRAN A., LEE M. P., PADGETT M. J., COOPER J. M. and DI LEONARDO R., *Phys. Rev. Lett.*, **108** (2012) 240601
- [27] KOUMAKIS N. and DI LEONARDO R., *Phys. Rev. Lett.*, **110** (2013) 174103
- [28] KOTAR J., DEBONO L., BRUOT N., BOX S., PHILLIPS D., SIMPSON S., HANNA S. and CICUTA P., *Phys. Rev. Lett.*, **111** (2013) 228103
- [29] SOKOLOV Y., FRYDEL D., GRIER D. G., DIAMANT H. and ROICHMAN Y., *Phys. Rev. Lett.*, **107** (2011) 158302
- [30] SASSA Y., SHIBATA S., IWASHITA Y. and KIMURA Y., *Phys. Rev. E*, **85** (2012) 061402
- [31] MARTÍNEZ I. A., ROLDÁN É., PARRONDO J. M. R. and PETROV D., *Phys. Rev. E*, **87** (2013) 032159
- [32] SOLANO R., BELLON L., PETROSYAN A. and CILIBERTO S., *Eur. Phys. Lett.*, **89** (2010) 60003
- [33] DOI M. and EDWARDS S. F., *The Theory of Polymer Dynamics* (Clarendon, Oxford) 1986
- [34] ZWANZIG R., *Nonequilibrium Statistical Mechanics* (Oxford University Press) 2001
- [35] SEKIMOTO K., *Prog. Theor. Phys. Suppl.*, **130** (1998) 17